Composite Temperature Record from the Greenland Summit, 1987–1994: Synthesis of Multiple Automatic Weather Station Records and SSM/I Brightness Temperatures

C. A. SHUMAN,* M. A. FAHNESTOCK,+ R. A. BINDSCHADLER,* R. B. ALLEY,@ AND C. R. STEARNS**

*Laboratory for Hydrospheric Processes, Oceans and Ice Branch (NRC-RRA), NASA/Goddard Space Flight Center, Greenbelt, Maryland
+Joint Center for Earth System Science, Department of Meteorology, University of Maryland, College Park, Maryland
@Earth System Science Center, The Pennsylvania State University, University Park, Pennsylvania
**Space Science and Engineering Center, University of Wisconsin, Madison, Wisconsin

(Manuscript received 21 September 1995, in final form 4 December 1995)

ABSTRACT

Air temperature (T_A) records from automatic weather stations (AWS) in central Greenland and associated Special Sensor Microwave/Imager (SSM/I) brightness temperature (T_B) data (37 GHz, vertical polarization) have been used to create a composite, daily, monthly, and annual average temperature record of the Greenland summit for the period 1987–1994. The record is derived primarily from near-surface temperatures from a single station; AWS Cathy (May 1987 to May 1989), which was moved 28 km and became AWS Kenton (starting in June 1989 and continuing). The Cathy daily average T_A record has been converted to the equivalent basis of Kenton by a technique based on the ratio of the contemporaneous daily average T_B data from the two locations. The accuracy of this technique has been statistically tested using 16 months of contemporaneous T_A and T_B data from the GISP2 and Kenton AWS. The resulting composite temperature record provides a multiyear dataset for comparison to other climate records from the Greenland summit.

1. Introduction

Long-term, automatic weather station (AWS) temperature records document meteorological variables of critical importance in this era of concern over climatic change. Establishment and maintenance of AWS across remote polar ice sheets is an especially critical project due to the climatic sensitivity of these areas. However, due to extreme conditions, near-surface observations from ice sheet locations are occasionally incomplete for significant periods of time. These discontinuities in an AWS temperature (T_A) record can be minimized through the use of satellite passive microwave brightness temperatures (T_B). The T_B data can be used to convert T_A data from nearby stations to an "equivalent basis" and thereby accurately complete gaps in critical temperature records. In addition, T_B data can also be used to fill short gaps in T_A records, without additional T_A data from a second site, although with comparatively reduced accuracy (Shuman et al. 1995a).

Using available T_A records from the University of Wisconsin's AWS network in central Greenland (see Fig. 1 and Table 1) (Stearns and Weidner 1991) and associated Special Sensor Microwave/Imager (SSM/I) 37-GHz, vertical polarization (V) T_B records from the National Snow and Ice Data Center (NSIDC), a nearly continuous temperature record for the Greenland summit has been synthesized for the period 1987–1994. The record discussed here consists primarily of daily average temperatures from a single station, AWS Cathy, which was relocated 28 km west and became AWS Kenton in late spring 1989 (see Fig. 2) (Weidner and Stearns 1991). The temperature data from AWS Cathy have been adjusted to the equivalent basis of AWS Kenton as have additional data from AWS Barber to produce the final composite record. This paper presents the details of the T_B ratio adjustment technique, which compensates for the distance and elevation differences between the AWS (see Table 2) under certain circumstances and thus allows creation of a nearly continuous multiyear temperature record from central Greenland. A record of this type can be used to calibrate general circulation model results from the Greenland summit as well as to be compared to stable isotope temperature proxy records.

2. Statement of problem

As the trend in Fig. 2 illustrates, the original temperature records from central Greenland are not continuous. The observed air temperature record is composed of multiyear segments from disparate AWS, and individual station records can contain temporal gaps of considerable length. This complicates efforts to establish a continuous temperature record in this area suitable for long-term climate monitoring. Unfortunately,

Corresponding author address: C. A. Shuman, Mail Code 971, Building 22, Room 260, NASA-Goddard Space Flight Center, Greenbelt, MD 20771.
E-mail: shuman@hardy.gsfc.nasa.gov

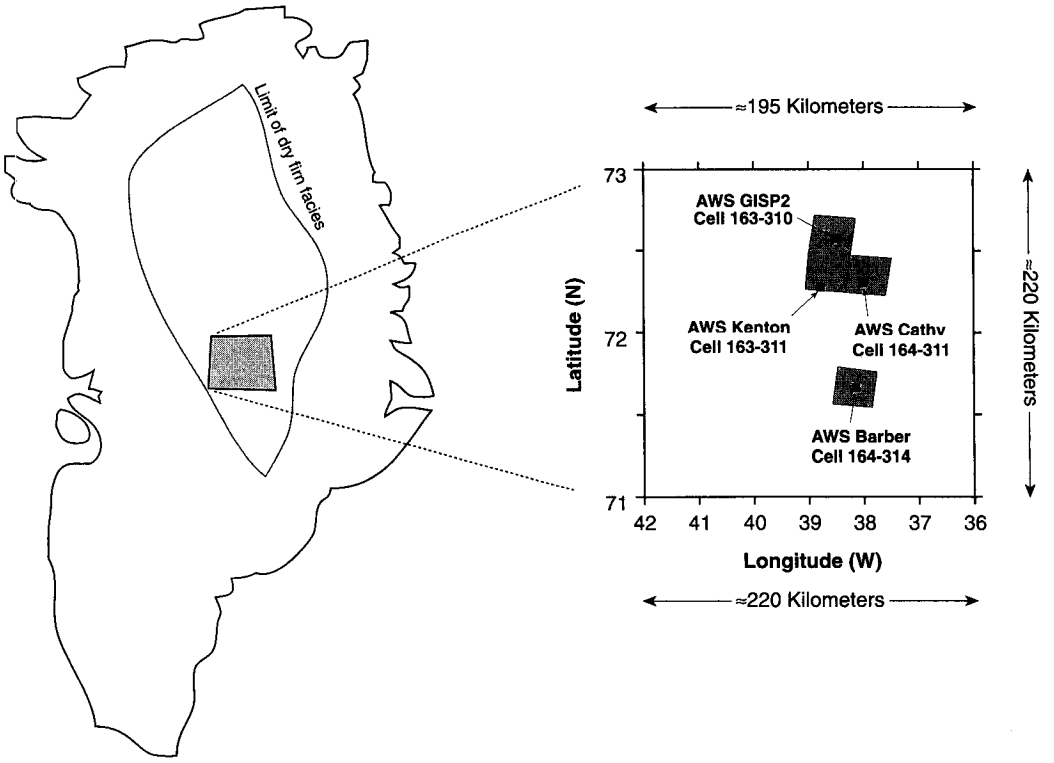

FIG. 1. Location map of University of Wisconsin automatic weather stations and corresponding National Snow and Ice Data Center SSM/I grid cells used in this study relative to the Greenland Ice Sheet Project 2 site at the Greenland summit. The limit of dry firn is after Benson (1982).

it is precisely in the polar regions that the possible effects of global climate change could produce the most dramatic changes and, thus, be most easily detected (Barron 1995). For this reason, it is important to combine the existing T_A records to develop a long-term temperature history for the Greenland summit.

Satellite passive microwave brightness temperatures are an effective surrogate temperature indicator in this region and can be used to define near-surface temperature trends (Shuman et al. 1995a). However, they do not provide a pure temperature signal; it is damped by the emission characteristics of the near-surface snow and ice. Satellite brightness temperature is primarily a function of the physical temperature of the near-surface snow multiplied by its emissivity. Atmospheric effects on brightness temperature can be effectively discounted due to the low temperatures and limited water vapor content found in this area (Maslanik et al. 1989). Emissivity is controlled primarily by radiative scattering from the ice grains over a skin depth of a meter or so for the 37-GHz channels but is dominated by the top few tens of centimeters (Rott et al. 1993) or about the depth of effect of the diurnal temperature cycle (Alley et al. 1990). The emissivity of the snow and ice is controlled primarily by grain size (Chang et al. 1976; Armstrong et al. 1993), which varies over an annual period (Benson 1962). This means that T_B data cannot be used directly to substitute for missing T_A data. However, as this paper will demonstrate, T_B data can be used to reliably adjust nearby AWS T_A records to the equivalent basis of an incomplete, but critical, T_A record thereby extending or completing it.

TABLE 1. Summary of the Greenland Summit network AWS used in this study.

Name	Latitude (°N)	Longitude (°W)	Elevation (m)	Start/stop date
Barber	71.67	38.17	3170	7/90
Cathy	72.30	38.00	3210	5/87–5/89
Kenton	72.28	38.82	3185	6/89
GISP2	72.58	38.46	3205	6/89

3. Methodology

The relationship of brightness temperature to physical temperature is described by the Rayleigh–Jeans approximation (Hall and Martinec 1985):

$$T_B = \epsilon T_A, \quad (1)$$

where ϵ is the emissivity of the near-surface snow and ice over the effective emission depth of the 37-GHz V microwave signal. The near-surface snow temperature

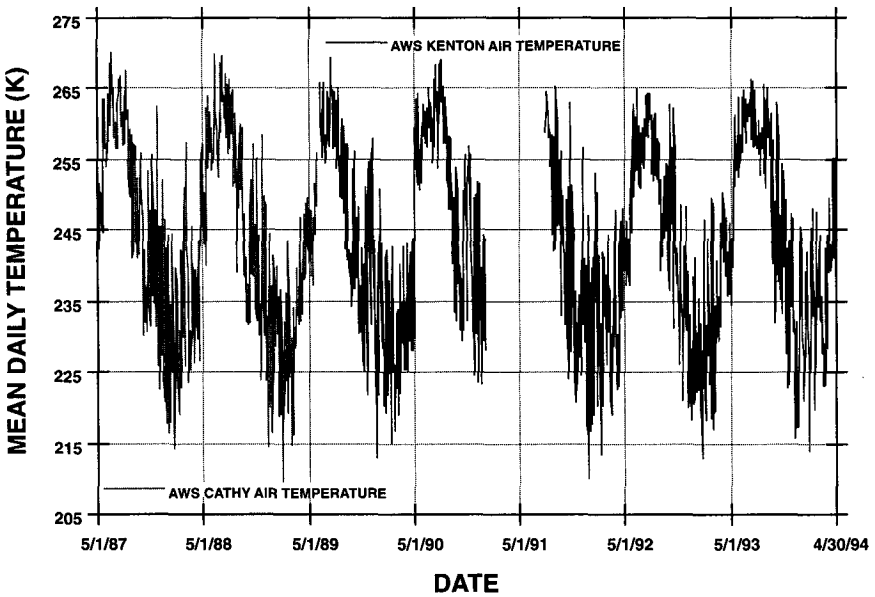

FIG. 2. Illustration of the best available multiyear temperature records at the Greenland summit from near-surface automatic weather station records.

is assumed in this case to be strongly controlled by the near-surface air temperature [a reasonable assumption, as demonstrated in Shuman et al. (1995a)]. If the emissivities for the two AWS sites to be merged are assumed to be approximately equal, then from Eq. (1) for each site

$$\frac{T_{B1}}{T_{B2}} = \frac{T_{A1}}{T_{A2}}, \tag{2}$$

where the numeric subscripts indicate the temperature information from the two AWS locations. If this is the case, then the contemporaneous ratios of brightness temperature and the air temperature should be equivalent. This can be illustrated over the summit region using T_A and T_B data from the GISP2 and Kenton AWS during 16 months from 1989–1990 (see Fig. 3). Although there are differences, most significantly in the relative ranges of the two ratios because of larger daily variability in air temperature, the trends of the two ratios are generally similar over the time period. Thus, the long-term trends of T_A and T_B ratio for these two sites justifies the assumption above and allows AWS record T_{A2} to be converted to the equivalent basis (eb) of T_{A1}:

TABLE 2. Elevation differences (m) and distances (km) between Summit network AWS.

Name	Barber	Cathy	Kenton	GISP2
Barber		40 m	15 m	35 m
Cathy	71 km		25 m	5 m
Kenton	72 km	28 km		20 m
GISP2	102 km	35 km	36 km	

$$\text{eb}T_{A1} = T_{A2}\left(\frac{T_{B1}}{T_{B2}}\right). \tag{3}$$

This is the approach that will be used to convert the AWS Cathy temperature record to the equivalent basis of AWS Kenton record. Although the T_A and T_B ratio assumption cannot be tested for Cathy and Kenton because of the lack of overlapping T_A records, it is assumed that the same general relationship holds across the 28 km from AWS Cathy to AWS Kenton as it does across the 36 km from AWS GISP2 to AWS Kenton (see Table 2). This assumption will be discussed further later in this paper.

The AWS data were obtained from the 3-h files at the anonymous ftp site operated by the University of Wisconsin—Madison (uwaaws.ssec.wisc.edu). These data are quality-controlled averages of 10-min AWS observations that are also available from this site. Daily average temperature values are then calculated from the 3-h data for comparison to the daily average passive microwave T_B required by this approach. [Detailed information on the AWS units used in Greenland, including data transmission and quality control, is presented in the Stearns et al. (1993) discussion of the Antarctic AWS network. This reference also specifies the resolution of the AWS temperature sensors as 0.125°C.]

The passive microwave data used in this study were subset from NSIDC CD-ROMs (NSIDC 1992). Daily averaged, 37-GHz V T_B from the SSM/I (*F8* and *F11*) for the 25 km × 25 km grid cells covering the AWS (see Fig. 1) are derived from the CD-ROMs and compiled for each site. The measurement accuracies of the 37-GHz V channels on

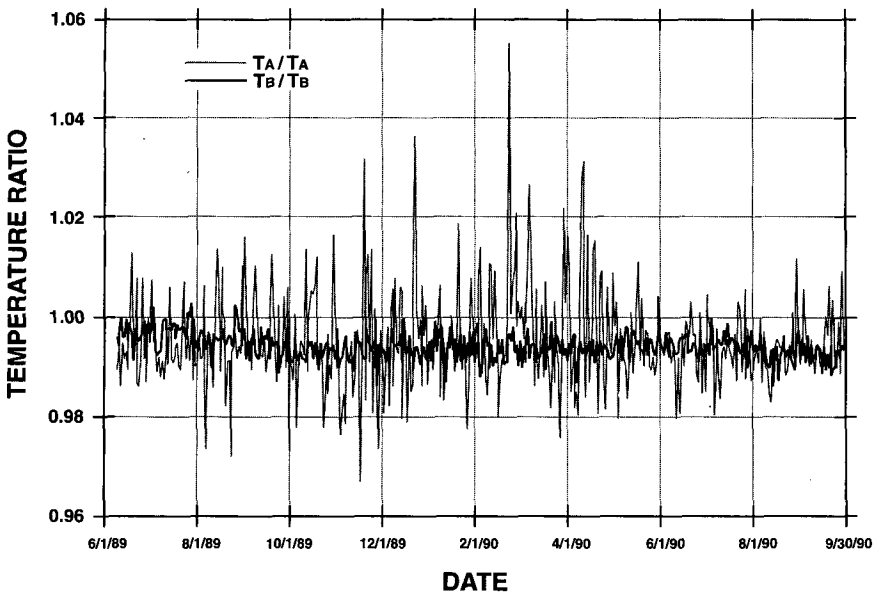

FIG. 3. Comparison of T_B/T_B and T_A/T_A ratio trends for the GISP2 and Kenton AWS sites. The general similarity of their trends justifies a key assumption used in the equivalent-basis technique.

these instruments are ±2 K (Hollinger et al. 1990). The relationship of 37-GHz V T_B data to near-surface AWS air temperatures is described in Shuman et al. (1995a). That paper details a technique that uses short-term AWS temperature and temporally equivalent T_B data to calibrate a modeled emissivity cycle. The modeled emissivity cycle can then be used to convert the T_B data into an estimated near-surface air temperature (T_C) with an accuracy typically better than a few K over monthly smoothing lengths. The 37-GHz V data are used in both that technique and this approach because they appear to have the best statistical correlation of the available long-term passive microwave channels with the mean daily air temperature data from the AWS (Shuman et al. 1995a).

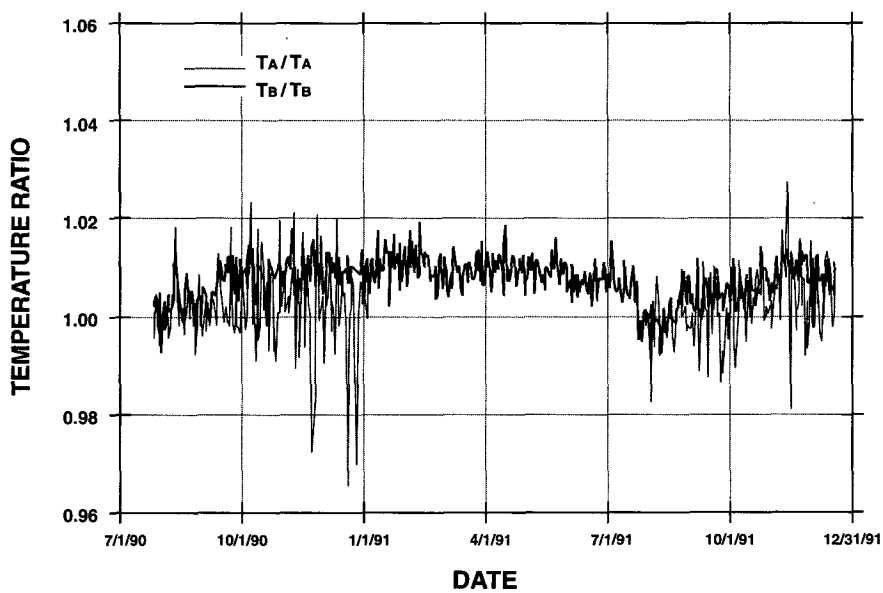

FIG. 4. Comparison of T_B/T_B and T_A/T_A ratio trends for the Barber and Kenton AWS sites. The similarity of their trends allows the Barber data to be incorporated by the equivalent-basis technique into the Kenton record to fill a data gap of almost 7 months (4 January to 26 July 1991).

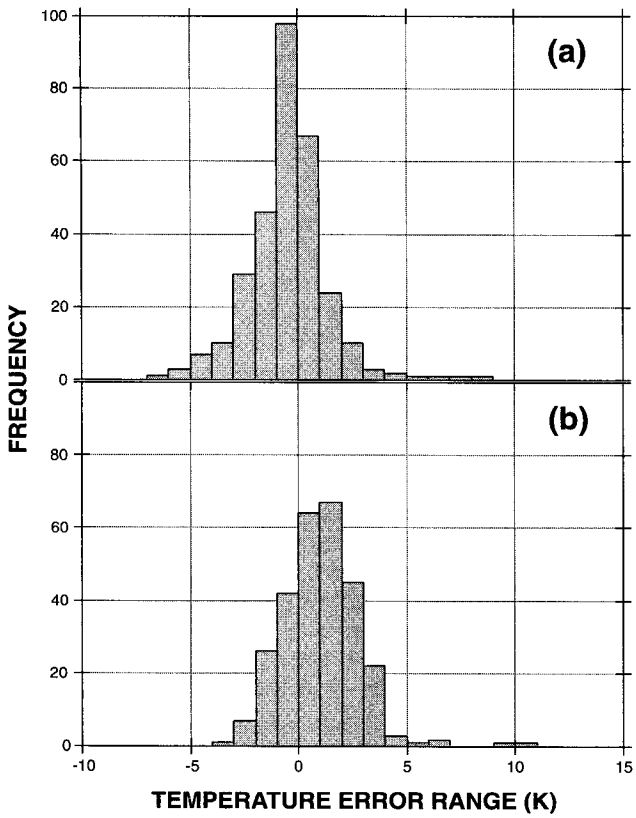

FIG. 5. Histogram of mean daily difference errors between (a) the observed AWS Kenton T_A data and the observed AWS Barber T_A data and (b) the observed AWS Kenton T_A data and the AWS Barber equivalent-basis T_A data over the time period illustrated in Fig. 4 (6 July 1990 to 18 December 1991 or 511 days with 282 observations). This shows that the technique does not improve the distribution mean (−0.421 to 1.037 K) but does improve the standard deviation slightly (1.816 to 1.799 K). This suggests that the technique is probably at the limit of its effective range.

Brightness temperature data from a 37-GHz *V* (0.81-cm wavelength) channel are available from SSM/I sensors starting with the *F-8* in July 1987 to December 1991. Data from additional sensors, with the *F-11* sensor starting in December 1991, are available from the NSIDC in the same general format as the data from the *F-8*. The relationship between these two sensor's 37-GHz *V* data has been studied over Greenland (Abdalati et al. 1995), and only very small differences appear to exist between the two datasets. The SSM/I *F-8* record from early December 1987 into mid-January 1988 is missing due to sensor malfunction (Hollinger et al. 1990).

4. Composite record development

As suggested by Fig. 2, the major obstacles to the completion of the composite AWS Kenton record are the adjustment of the AWS Cathy record (May 1987 to May 1989) and the completion of the AWS Kenton record across a period of missing data (January 1991 to July 1991). Secondary obstacles are presented by the lack of SSM/I data during May 1987 to July 1987 and December 1987 to January 1988 as well as the data gap when AWS Cathy was being moved to become AWS Kenton. Variations on the method outlined above or discussed in Shuman et al. (1995a) will be used to account for these obstacles.

The largest gap in the AWS Kenton record (January 1991 to July 1991) was completed by the insertion of a contemporaneous air temperature record from AWS Barber (approximately 72 km south; see Fig. 1 and Table 2). The AWS Barber data were adjusted by the T_B ratio technique [Eq. (3)] and the results were assessed by analysis of available T_B and T_A data between the two sites over a 17-month period. Figure 4 indicates that the ratio trends during the months prior to and following the AWS Kenton data gap are not as similar as those compared in Fig. 3. Despite an increased difference between the ratio trends, the technique's necessary assumption still appears to be valid. Comparison of AWS Barber equivalent basis temperatures with actual observed AWS Kenton temperatures before and after the data gap (approximately 10 months of data) yields a histogram of daily difference errors (see Fig. 5b) with a mean difference of 1.037 K and a standard deviation of 1.799 K. The difference histogram between unconverted AWS Barber data and the AWS Kenton data has a mean of −0.421 K and a standard deviation of 1.816 K (see Fig. 5a). This suggests that converting the AWS Barber air temperature data by the equivalent basis technique produces only a marginal improvement in the standard deviation and actually reduces the accuracy of the overall distribution. This result will be discussed further below.

Two portions of the AWS Cathy record required additional processing before these data could be converted to the equivalent basis of AWS Kenton using Eq. (3). First, the AWS Cathy record began before the SSM/I *F-8* was launched (May 1987 vs July 1987), and, second, there was a period during the AWS Cathy record when the SSM/I sensor was not operating (December 1987 to January 1988). As a result, the 37-GHz *V* T_B ratio between the two sites during these periods had to be synthesized. This was accomplished using the software package Igor® 1.26, which generated an annual sinusoid model from later T_B ratio data. Despite apparently decreased sensitivity in these modeled T_B ratios relative to actual ratios (see Table 3), this allowed conversion of the Cathy T_A record from its start date. As noted above, the lack of contemporaneous T_A records from both sites prevents direct assessment of temperature errors; however, it is assumed that they are similar to those observed between AWS GISP2 and AWS Kenton. The distribution of daily difference errors between GISP2 and Kenton (see Fig. 6b) has a mean difference of 0.273 K and a standard deviation of 1.637 K. In this case, the difference histogram between the unconverted AWS Kenton data and the AWS GISP2 data has a mean and standard deviation of −1.184 K and 2.286 K, respectively (see Fig. 6a). This

TABLE 3. Estimates of daily temperature errors for segments of the composite record.

Composite segment(s)	Segment dates (day/mo/yr)	Estimated error (±) (K)
[1]AWS Cathy eb T_A^*	5/4/87–7/9/87 and 12/3/87–1/13/88	2.424
[2]AWS Cathy eb T_A	7/10/87–12/2/87 and 1/14/88–5/29/89	1.637
[3]Modeled T_B/T_A	5/30/89–6/6/89	5.614
[4]AWS Kenton obs T_A	6/9/89–1/3/91 and 7/27/91–12/31/93	0
[5]AWS Barber eb T_A	1/4/91–7/26/91	1.799

[1] Estimated as equal to the standard deviation of the GISP2 − Kenton comparison (Fig. 6) exaggerated by the standard deviation of the absolute difference between the observed and modeled T_B/T_B ratios during the periods when SSM/I data was unavailable.
[2] Estimated as equal to the standard deviation of the GISP2 − Kenton comparison (Fig. 6).
[3] Estimated as equal to the average standard deviation produced by the approximate emissivity modeling technique (see Shuman et al. 1995a).
[4] Values are the mean of observed temperatures at Kenton, which are accurate to ±0.125 K.
[5] Estimated as equal to the standard deviation of the Kenton − Barber comparison (Fig. 5).

suggests that converting the AWS Kenton air temperature data by the equivalent basis technique produces substantial improvements in the standard deviation and mean of the difference distribution.

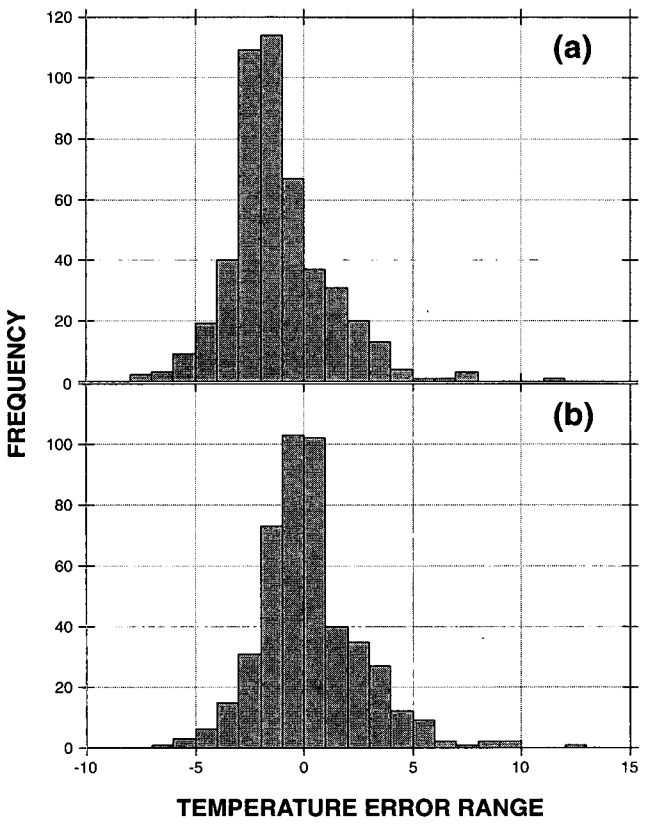

FIG. 6. Histogram of mean daily difference errors between (a) the observed AWS GISP2 T_A data and the observed AWS Kenton T_A data and (b) the observed AWS GISP2 T_A data and the AWS Kenton equivalent-basis T_A data over the time period illustrated in Fig. 3 (9 June 1989 to 30 September 1990 or 479 days with 465 observations). This shows that the technique improves the distribution mean (−1.184 to 0.273 K) as well as the standard deviation (2.286 to 1.637 K). This suggests that the technique is within its effective range.

The improved mean and standard deviation of the GISP2 − Kenton differences (see Fig. 6) relative to the Kenton − Barber differences (see Fig. 5) is presumed to reflect the previously observed closer association of the T_B and T_A ratios between the two AWS pairs (see Figs. 3 and 4). This suggests that emissivity variability in this area, as demonstrated by Chang et al. (1976), may reach a critical threshold as the distance between the AWS sites increases. If so, then the equivalent-basis technique for the conditions considered here may be at its effective limit at distances of about 70 km but may be quite suitable over the distances between GISP2 and Kenton (36 km) and, therefore, by extension, between Cathy and Kenton (28 km). This suggests that it should be possible to synthesize accurate temperature records for locations at about this range from an operating AWS (one SSM/I grid space or 25 km) if the T_B ratio trend can be generated. This may be important at ice sheet sites with a central camp and peripheral activities that lie a few tens of kilometers from the AWS. Outliers in the two histograms (see Figs. 5 and 6) are probably the result of local meteorological variability (clouds in one area vs sun at the other) as well as possibly uneven SSM/I data collection. [The satellite carrying the SSM/I has an orbit of approximately 102 min. (Hollinger et al. 1990) and at these latitudes the daily average 37-GHz V value may be based on one to perhaps six orbits through the course of the day and multiple observations that are binned into each grid cell during each orbit.]

The final gap in the composite record resulted from the move of AWS Cathy to the site of AWS Kenton (30 May 1989 to 6 June 1989). This data gap was filled through the use of the emissivity modeling technique based on the Raleigh–Jeans approximation outlined in Shuman et al. (1995a). A 500-day record centered on the gap was taken from the combined AWS Kenton and equivalent basis AWS Cathy T_A data and used with the 37-GHz T_B from the Kenton site to model the emissivity during this time period. The modeled emissivity cycle was then used with the T_B data from the same time period to generate the temperature estimates used

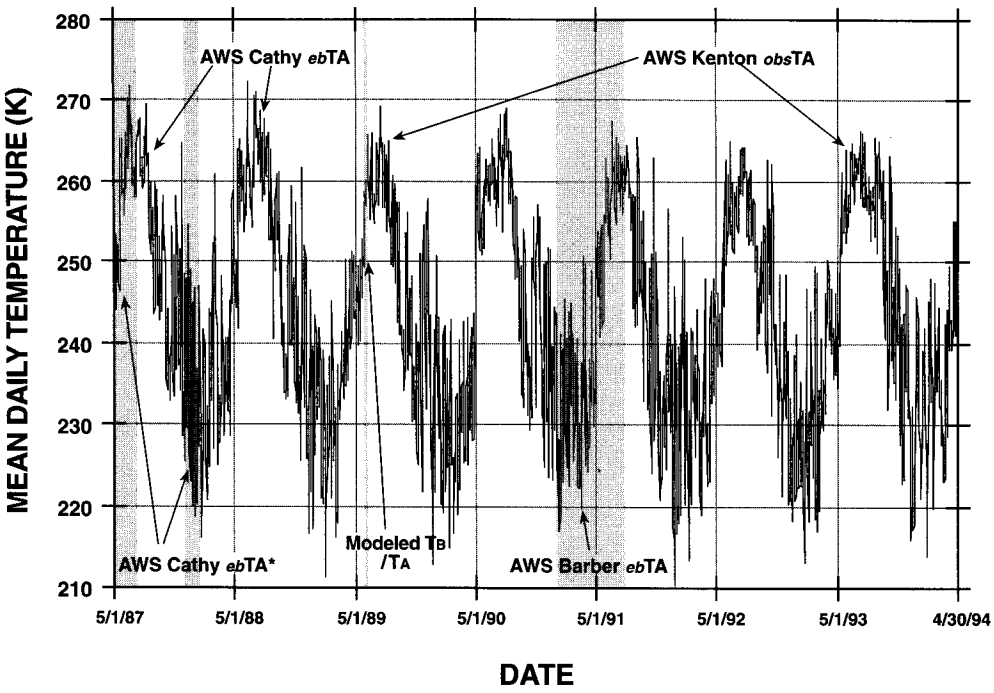

FIG. 7. Composite mean daily temperature record from AWS Kenton at the Greenland summit. The gray boxes define the portions of the record that required the special handling and are described further in the text. Labels and arrows are used to indicate the data source for all major components of the composite record. Note the general pattern of primary and secondary maxima and minima over the period of record.

to fill the gap [see Shuman et al. (1995a) for a complete discussion of the technique]. Although this short period of data lacks the same sensitivity as the equivalent basis records (see Table 3), it is included here to make the composite record complete.

5. Discussion

The end product is the daily average temperature record presented in Fig. 7. The components of the record are detailed in Table 3 along with estimates of the standard deviation of their error distribution as well. Overall, the record is more than 98% complete with a few short gaps that are mostly due to brief periods of missing SSM/I data during the AWS Cathy portion of the record. A table of data giving details of the record is available upon request.

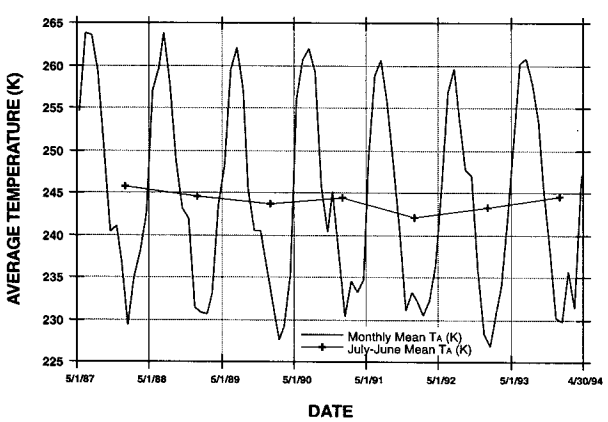

FIG. 8. Mean monthly and mean annual temperature trends for AWS Kenton. Note the decreased mean annual temperature for the year following the Mt. Pinatubo eruption in June 1991 and the subsequent 2.5 K rise in the years afterward.

The record over the 7 years presented here appears to be one of highs in 1987 and 1988 (Lyon and Dole 1995) followed by gradual summer cooling until 1992 with no clear winter pattern. The daily average temperature record also illustrates a characteristic feature of the summit temperature record. The annual temperature cycle in this region has the typical summer and winter primary maxima and minima as well as a secondary maxima and minima in the fall to early winter. This secondary warm peak typically consists of one or more events that may warm the summit region by as much as 20 K over a period of a week to several weeks (see Fig. 7). They occur primarily during October and November but may sometimes occur in early January. Other, shorter duration warm periods, or "spikes," may occur through the winter cool period (see Fig. 7). Based on analysis of Genesis GCM simulations (see Thompson and Pollard 1995), this appears to be the result of poleward advection of warmer air masses and the resultant trapping of longwave IR radiation (P. Fawcett 1995, personal communication). These secondary temperature maxima appear consistently in sta-

ble isotope profiles ($\delta^{18}O$ and δD) from this region (Shuman et al. 1995b), suggesting that they are associated with significant accumulation as well.

This secondary warm period is significant enough to appear in the monthly average temperature plot shown in Fig. 8, although it commonly appears less dramatically as a shoulder or break in slope instead of as a defined peak. The monthly mean and annual mean temperatures in Fig. 8 support the impression of generally cooling summers with no clear winter pattern. The annual mean temperatures, plotted at the annual period midpoint, appear to reflect an approximate 2.5 K cooling that may be associated with the major eruption of Mt. Pinatubo during 15–16 June 1991 (J. Mao 1995, personal communication; McClelland et al. 1991). The annual average period, 1 July to 30 June, was chosen deliberately to accentuate possible post-Pinatubo cooling. Subsequent years, 1992–1994, indicate a gradual warming of equal magnitude, which may reflect the progressive fallout of Pinatubo's stratospheric dust (Robock and Mao 1995; Barron 1995).

6. Summary

Using a combination of surface and satellite temperature information, a multiyear temperature record for the Greenland summit region has been compiled. This composite record details seven years of daily average temperature history, characterizes distinctive aspects of the summit temperature cycle, and provides a basis for comparison to other records from this region. The equivalent-basis technique allows accurate integration of multiple AWS temperature records over limited geographic areas. This suggests that future ice sheet research sites could benefit from the operation of multiple AWS to ensure that a complete temperature record can be obtained. In addition, the technique suggests that accurate air temperature records can be synthesized for locations adjacent to an operating AWS (within tens of kilometers) if the brightness temperature data are available from both sites. Finally, the resulting mean annual temperature data suggests that the major eruption of Mt. Pinatubo in June of 1991 may have cooled this region by more than 2 K.

Acknowledgments. We thank the GISP2-SMO, 109th ANG, and PICO, for their logistics support and Peter J. Fawcett, Jianping Mao, and two anonymous reviewers for their technical support. This work was performed while the first author held a National Research Council Associateship at NASA/Goddard Space Flight Center.

REFERENCES

Abdalati, W., C. Otto, K. Steffen, and K. C. Jezek, 1995: Comparison of brightness temperatures from SSM/I instruments on the DMSP F8 and F11 satellites for Antarctica and the Greenland ice sheets. *Int. J. Remote Sens.*, **16,** 1223–1229.

Alley, R. B., E. S. Saltzman, K. M. Cuffey, and J. J. Fitzpatrick, 1990: Summertime formation of depth hoar in central Greenland. *Geophys. Res. Lett.*, **17,** 2393–2396.

Armstrong, R. L., A. T. C. Chang, A. Rango, and E. Josberger, 1993: Snow depths and grain-size relationships with relevance for passive microwave studies. *Ann. Glac.*, **17,** 171–176.

Barron, E. J., 1995: Global change researchers assess projections of climate change. *Eos, Trans. Amer. Geophys. Union,* **76,** 185–190.

Benson, C. S., 1962: Stratigraphic studies in the snow and firn of the Greenland Ice Sheet. Res. Rep. 70, U.S. Army, SIPRE (now CRREL). 93 pp. plus 3 appendixes. [Available from CRREL, Hanover, NH 03755.]

Chang, A. T. C., P. Gloersen, T. T. Wilheit, and H. J. Zwally, 1976: Microwave emission from snow and glacier ice. *J. Glac.,* **16,** 23–39.

Hall, D. K., and J. Martinec, 1985: *Remote Sensing of Snow and Ice.* Chapman and Hall, 189 pp.

Hollinger, J. P., J. L. Pierce, and G. A. Poe, 1990: SSM/I instrument evaluation. *IEEE Trans. Geosc. Remote Sens.*, **28,** 781–790.

Lyon, B., and R. M. Dole, 1995: A diagnostic comparison of the 1980 and 1988 U.S. summer heat wave droughts. *J. Climate,* **8,** 1658–1675.

Maslanik, J. A., J. R. Key, and R. G. Barry, 1989: Merging AVHRR and SMMR data for remote sensing of ice and cloud in polar regions. *Int. J. Remote Sens.*, **10,** 1691–1696.

McClelland, L., D. Lescinsky, and M. Slaboda, 1991: Pinatubo. *Bull. Global Volc. Net.,* **16,** 2–8.

NSIDC, 1992: DMSP SSM/I brightness temperature and sea ice concentration grids for the polar regions. CD-ROM user's guide. National Snow and Ice Data Center, Special Rep.—1, Cooperative Institute for Research in Environmental Sciences. [Available from CIRES, University of Colorado, Boulder, CO 80309.]

Robock, A., and J. Mao, 1995: The volcanic signal in surface temperature observations. *J. Climate,* **8,** 1086–1103.

Rott, H., K. Sturm, and H. Miller, 1993: Active and passive microwave signatures of Antarctic firn by means of field measurements and satellite data. *Ann. Glaciol.,* **17,** 337–343.

Shuman, C. A., R. B. Alley, S. Anandakrishnan, and C. R. Stearns, 1995a: An empirical technique for estimating near-surface air temperatures in central Greenland from SSM/I brightness temperatures. *Remote Sens. Environ.,* **51,** 245–252.

——, ——, ——, J. W. C. White, P. M. Grootes, and C. R. Stearns, 1995b: Temperature and accumulation at the Greenland summit: Comparison of high-resolution isotope profiles and satellite passive microwave brightness temperature trends. *J. Geophys. Res.,* **100**(D5), 9165–9177.

Stearns, C. R., and G. A. Weidner, 1991: The polar automatic weather station project of the University of Wisconsin. *Proc. Int. Conf. on the Role of the Polar Regions in Global Change,* Vol. 1, Fairbanks, AK, Geophysical Institute, and Center for Global Change and Arctic System Research, 58–62.

——, L. M. Keller, G. A. Weidner, and M. Sievers, 1993: Monthly mean climatic data for Antarctic automatic weather stations. *Antarctic Meteorology and Climatology: Studies Based on Automatic Weather Stations,* Vol. 61, *Antarctic Res. Ser.,* D. H. Bromwich and C. R. Stearns, Eds., Amer. Geophys. Union, 1–21.

Thompson, S. L., and D. Pollard, 1995: A global climate model (GENESIS) with a land-surface transfer scheme (LSX). Part I: Present climate simulation. *J. Climate,* **8,** 732–761.

Weidner, G. A., and C. R. Stearns, 1991: A two-year record of the climate on the Greenland crest from an Automatic Weather Station. *Proc. Int. Conf. on the Role of the Polar Regions in Global Change,* Vol. 1, Fairbanks, AK, Geophysical Institute, and Center for Global Change and Arctic System Research, 220–222.